MIBS past present and future

J. Leijtens[1] , C.Hoegaerts[1],J.Barros[1], J.de Vries[2]
[1]) TNO Science and Industry, Stieltjesweg 1, 2628 CK Delft
Phone: +31 15 2692000, Fax: +31 15 2692111,
[2]) Dutch Space, Newtonweg 1, 2333 CP Leiden
Phone: +31 71 5245000, Fax: +31 71 5245999

ABSTRACT

The microbolometer spectrometer breadboard MIBS is a prism spectrometer that uses an uncooled microbolometer detector array and has been designed for the ESA EarthCARE mission. In order to demonstrate its feasibility a breadboard has been build, and tests have been performed that show good correlation between predicted and achieved results. Although application for EarthCARE has become uncertain due to geodistribution issues, it is feld that this instrument (which is small enough to give grown up performance to a micro satellite) has a lot of application potential for applications like weather forecasting and forest fire detection. The presentation will elaborate on performance predicted, measurements performed, results achieved and future applications.

1 INTRODUCTION

The microbolometer spectrometer is a prism spectrometer that uses a combination of reflective optics and a high speed camera in order to obtain an as high as possible NETD.
(Fig 2-1)

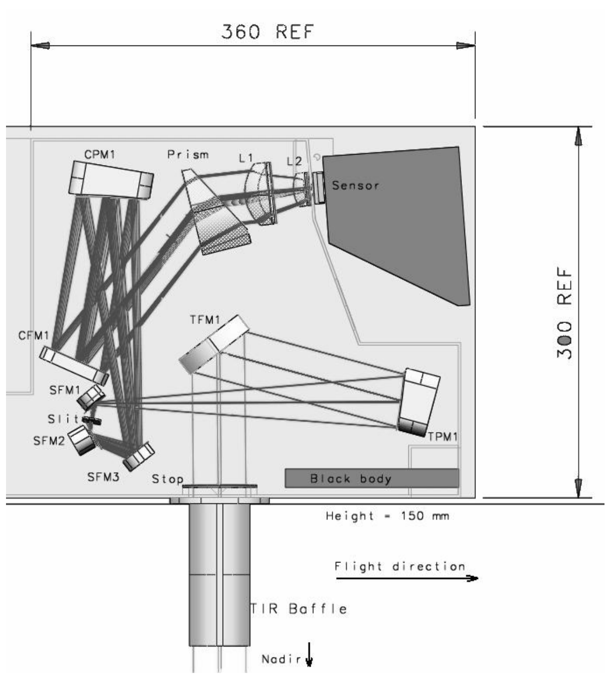

Fig 2-1 principle optical diagram of MIBS

Sensors, Systems, and Next-Generation Satellites XI
edited by Roland Meynart, Steven P. Neeck, Haruhisa Shimoda, Shahid Habib
Proc. of SPIE Vol. 6744, 674418, (2007) · 0277-786X/07/$18 · doi: 10.1117/12.735513

The nadir view is looking down in this picture, and the incoming radiation is deflected by TFM1 to the collimator TPM1 which focuses on the slit via compensation mirror SFM1. The slit image is again formed into a collimated beam via compensation mirror SFM2, fold mirror SFM3. collimation mirror CPM1 and fold mirror CFM1. The radiation is then dispersed by the prism and imaged on the detector via Germanium lenses L1 and L2. TFM1 is the calibration mirror which is used to point at either one of two blackbody's incorporated in the design or the scene. For this purpose the mirror of the MIBS breadboard can be rotated by means of a small stepper motor.

Given the close proximity of the parts CFM1,SFM1,slit and SFM2 (and the desire to assemble the entire system on basis of manufacturing tolerances as much as possible) a single mechanical assembly is created out of these parts. This so called slit assembly (fig 2-2) is used as the starting point of the alignment procedure.

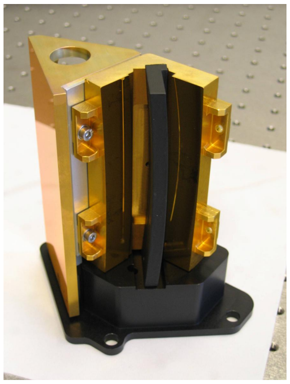

Fig 2-2 slit assembly

As will be shown later, this slit assembly plays an important role in the inherent properties of the instrument. (For a more elaborate description of the alignment procedure and pictures of the hardware see [Ref1])

2 CURRENT STATUS

The MIBS breadboard has been assembled and a number of measurements have been performed in order to verify the correct behaviour of the instrument.

- The detector was correctly aligned using a CO_2 laser and an integrating sphere.
- A first vignetting measurement of the system has been made.
- The influence of some key components that have been identified during the radiometric analysis has been verified.
- CTF measurements have been performed.
- Numerical analysis of the data has been performed to calculate the NETD of the system.

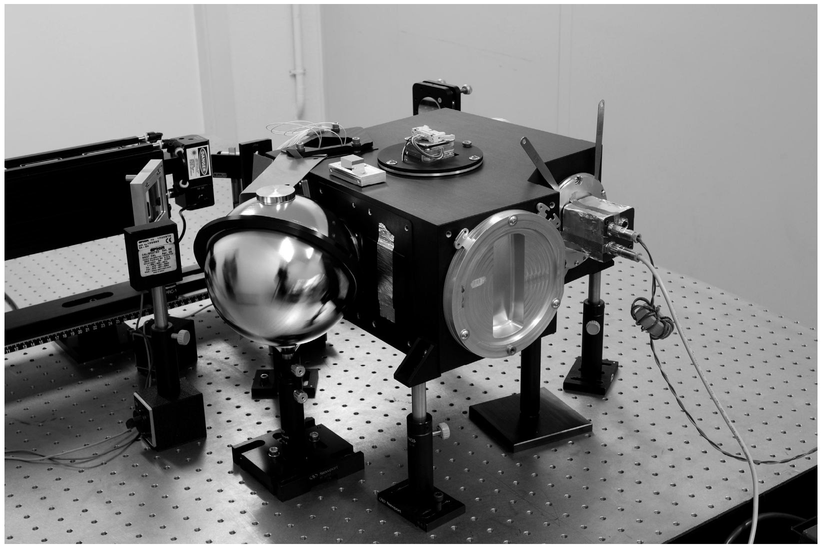

Fig 3-1 MIBS during laser alignment

2.1 Optical alignment of the detector.

The optical alignment of the detector was performed by a CO2 laser illuminating an integrating sphere. This was supposed to give a uniformly illuminated entrance pupil, but the intensity profile found indicated a large spatial non-uniformity over the field of view (fig 4.1-1). This was later on proven to be caused by laser speckle effects.(fig 4.1-2)

Fig 3.1-1 pixel values of one line during laser alignment over time

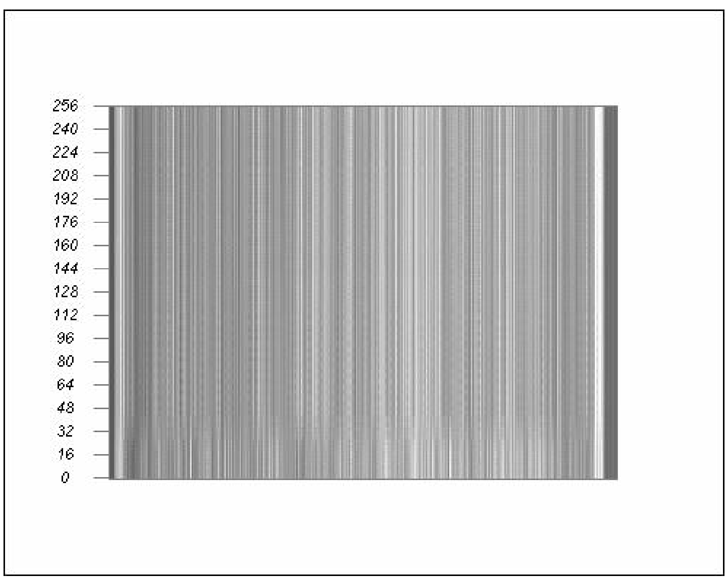

Vibrating the integrating sphere to scramble the speckle helped considerably as can be seen in fig 4.1-2. Therefore the final measurements where only taken while vibrating the sphere both manually and with a piezo motor at the same time.
Although not directly striking, fig 4.1-1 also shows another effect that was found during the alignment of the detector. The laser used shows some mode hopping behavior, meaning that after some time, the wavelength switches between

10.57 and 10.61 micrometer. This wavelength hop changes the speckle pattern as can be seen in the area of line 32. Since the actual laser mode is more or less stable, the mode hopping is more or less random and incontrollable. Although the speckle pattern is altered by the mode hopping, even after vibrating the sphere a noticeable signal intensity shift was noticed at occasions. This is believed to be caused by the combination of the monochromatic character of the radiation in combination with the limited fillfactor of the detectors. This effect can be used to discriminate sub slitfunction wavelength shifts in case the slitfunction is characterized and will allow MIBS to measure far smaller wavelength variations as compared to the slitfunction width which will be between 250 and 300 nm wide.

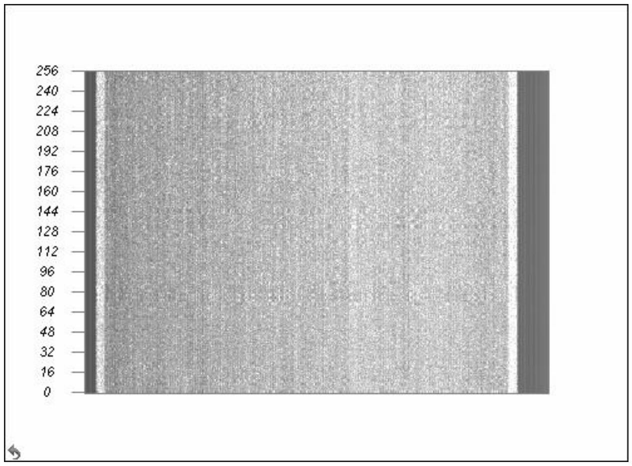

Figure 3.1-2: Picture showing reduced speckle due to vibration

The picture produced while shaking the integrating sphere (fig 3.1-2) shows that the detector shows some column effects which is understandable from the way the detector is build and readout.

The detector was aligned using the laser as described, and from fig 3.1-3 it can be seen that the alignment of the detector is more or less within one pixel.
For the final instrument this would need to be done more accurately, but due to the lack of real time signal processing and the simple mechanical interface it was not feasible to do this any better now within a reasonable timeframe. Nevertheless the picture show clearly that the image curvature correction is doing a good job although it has not be verified that the actual remaining curvature is less then one tenth of a pixel as predicted.

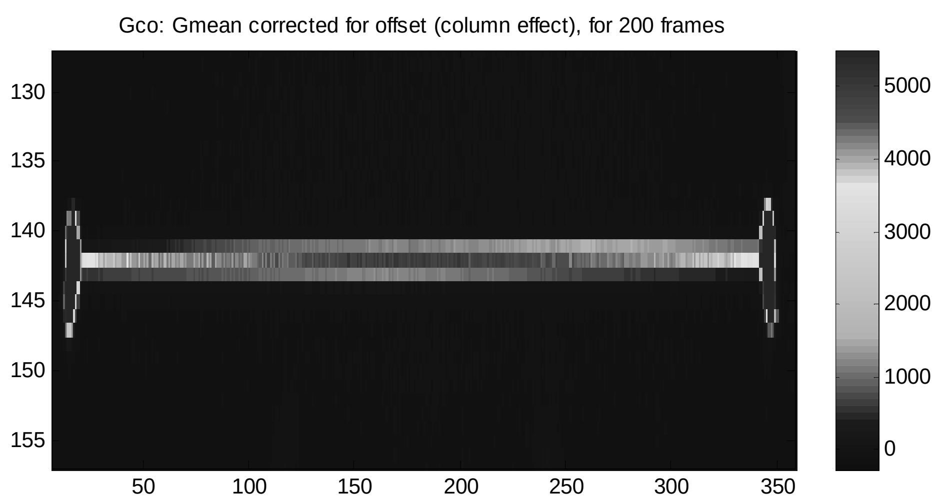

Figure 3.1-3: monochromatic picture showing detector alignment

2.2 Average intensity variation

As reported before [Ref1], a distinct intensity variation can be noticed when comparing one frame to the other. This intensity variation is having a distinct influence on the noise as calculated for the measurements, and therefore would need to be corrected. When looking at the polychromatic intensity plot (fig 3.1-3) it can be clearly seen that large area's directly adjacent to the image (red line with spikes) are unaffected by the (large) signal. These areas can be used for calculating the average scene intensity. There seems to be a ghost image in the left part of the image which is possibly caused by reflections at the prism surfaces (given the curvature) but this ghost occurs significantly outside the actual signal area and therefore would not be of great concern.

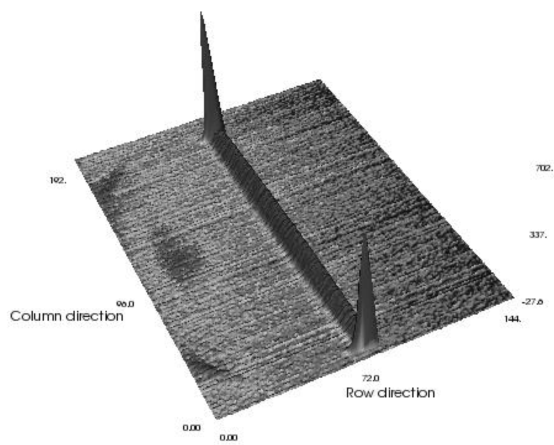

Figure 3.2-1: Polychromatic intensity plot with histogram color scale showing very low intensity effects

If the standard deviation (noise) on a single pixel with and without correction for the average scene intensity is calculated over 200 frames a significant reduction in noise can be observed as can be seen in fig 3.1-4. The difference is more striking if the actual standard deviation is calculated. Through the average signal compensation, the standard deviation for a non selected set of data was reduced from 5.62 to 4.02 which entails **a reduction of 28.5 %**

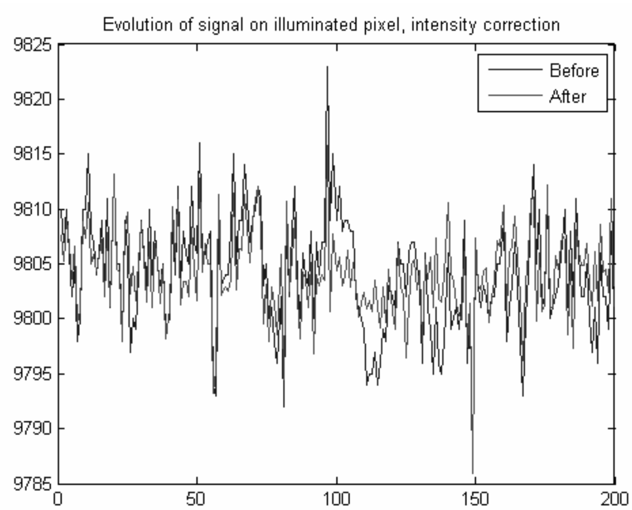

Figure 3.2-2: signal on pixel with and without average intensity compensation

2.3 Improved blackbody

The blackbody used to do the earliest measurements consisted of a simple black anodized aluminum plate with a heater and thermocouple attached to it. Although this heater produced a measurable signal, the radiation input to the MIBS breadboard probably had a significant deviation from the one expected due to the low emissivity of the blackbody. Since this lower radiation directly translates into a lower measured NETD, it was decided to build an calibrate a better blackbody to do the MIBS tests with.

The blackbody was characterized that the Dutch Measurements Institute NMI and showed good overall performance.

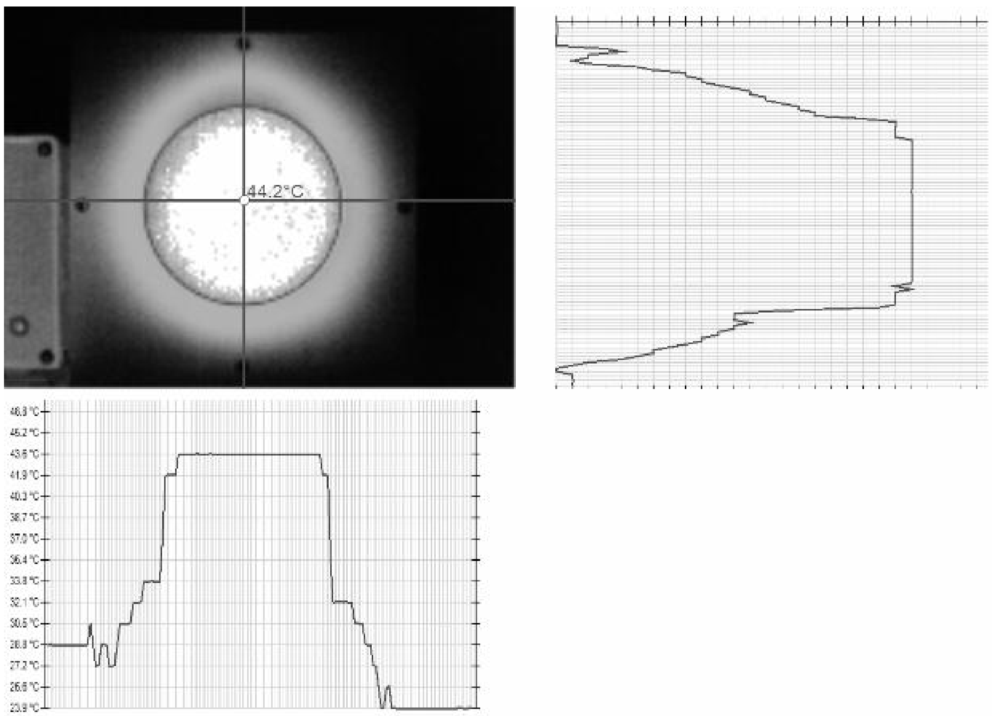

Figure 3.4-1: blackbody radiation temperature

Because the exit aperture of the blackbody is 60 mm and the entrance aperture of MIBS is 42.3 mm, the aperture of MIBS is completely filled and the radiation temperature is constant at 44.2 ±0.1˚C. This blackbody can therefore be considered fit to serve as a secondary standard.

2.4 Thermal stability measurements

When operating the breadboard it was noticed that the temperature of the breadboard increases steadily due to self heating (power dissipation in the bolometer camera). As part of the test program it was always foreseen to measure the influence of what where deemed the most critical parts in the instrument.

- Slit assembly
- Camera assembly
- Detector.

The detector temperature currently is not controlled by external means, and therefore the camera will drift with the breadboard temperature.
The slit assembly and the camera assembly however are equipped with dedicated heaters, allowing to heat these assemblies until they are significantly above the breadboard temperature.

Heating the slit up to a temperature 2 degrees above the breadboard temperature nicely shows which parts of the image are directly influenced by the slit.(fig 3.4-1)

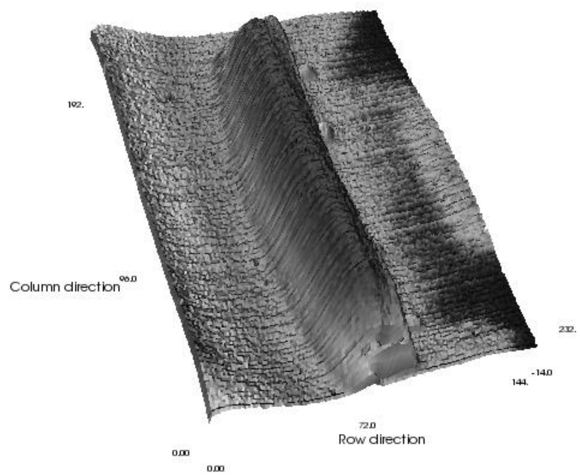

Figure 3.4-1: image with increased slit temperature 3D plot

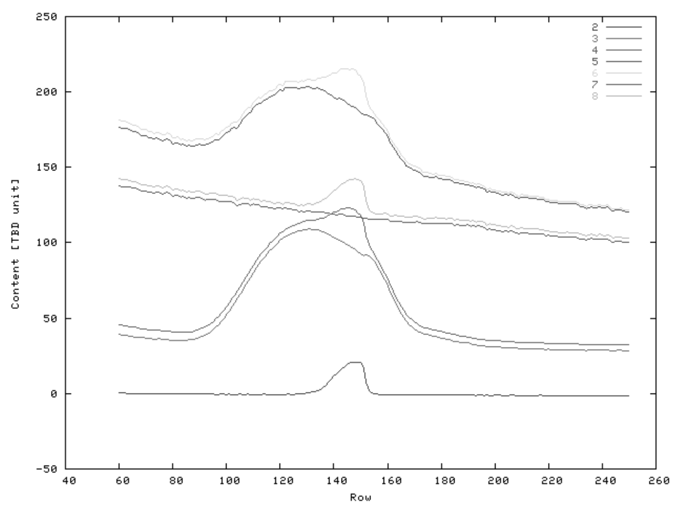

Figure 3.4-2: image with increased slit temperature graph

As can be clearly seen, the influence of 2 degrees slit temperature increase (big hump) is much more significant than the influence of 20 degrees input level decrease (small hump)

Another significant effect was predicted for the temperature increase of the camera assembly. It was expected that the signal would decrease due to increased absorption in the germanium. This behavior was confirmed by the measurements, but proved to be much more significant then expected. (fir 3.4-3)

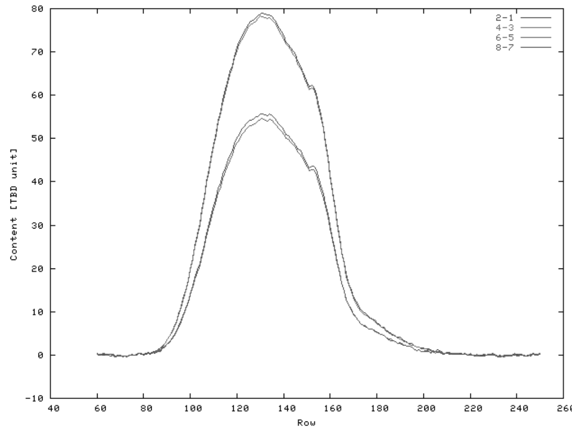

Figure 3.4-3: image with increased slit temperature at two camera temperatures

From the graph it can be seen that the signal decreased from 78 counts peak to 55 counts peak which is **a 29.5% decrease over 2 degrees centigrade.** Since the instrument, for the majority of the time, has been operated at temperatures significantly above room temperature, this is bound to have influence any NETD measurements that have been performed.

For the moment it is still unclear what causes this large signal attenuation as a function of temperature, but it is believed to be a combination of the absorption in the germanium and decrease in detector sensitivity.

As the original instrument concept called for a cold optical bench (-50˚C) this does hold promise for significant performance improvement when changing to lower operating temperatures (although the relative performance increase is expected to become less in case the detector is kept at room temperature).

The last item that one would like to control in temperature is the detector temperature, but this temperature is now directly controlled by the camera electronics and is out of control of TNO. There is however one effect which seems to be associated with the temperature increase of the detector assembly.

From the first beginning it was noticed that there is a distinct slope in the intensities when reading over one column (fig 3.4-4). From this graph it can clearly be seen that the actual signal, in the order of some counts per degree centigrade, is hidden in the overall signal which varies by some 500 counts over the image on top of an offset of some 10.000 counts.

In order to compensate for this, a background level is determined using the average of 200 measurements just outside the illuminated area (just above and below the illuminated area. When this background image is subtracted the signal becomes visible (fig 3.4-5).

It has been noted that all of this signal show a remnant of the original intensity profile. When this remnant is removed by means of curve fitting (between parts outside the illuminated area) the curves nicely fit.

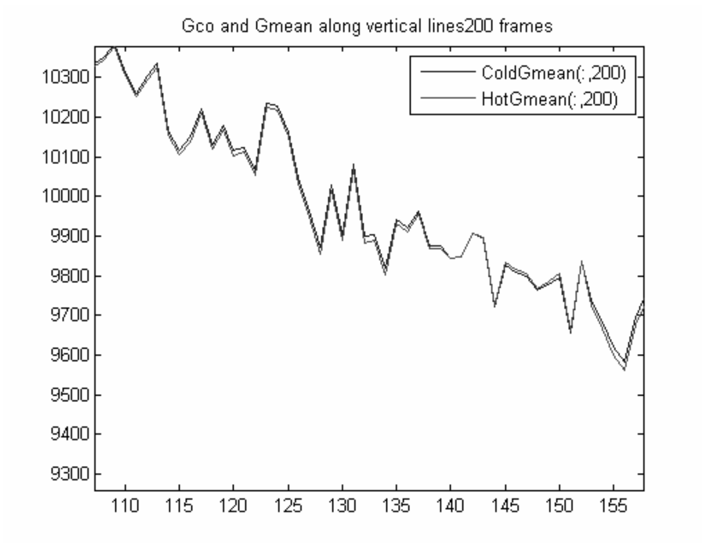

Figure 3.4-3: intensity variations over one line

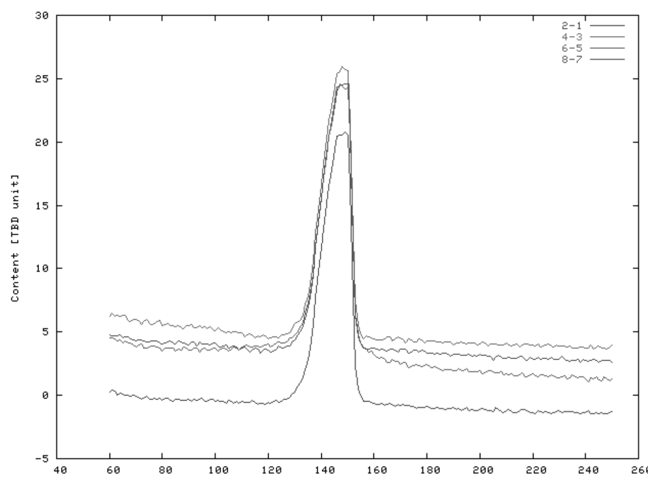

Figure 3.4-4: intensity variations after background subtraction

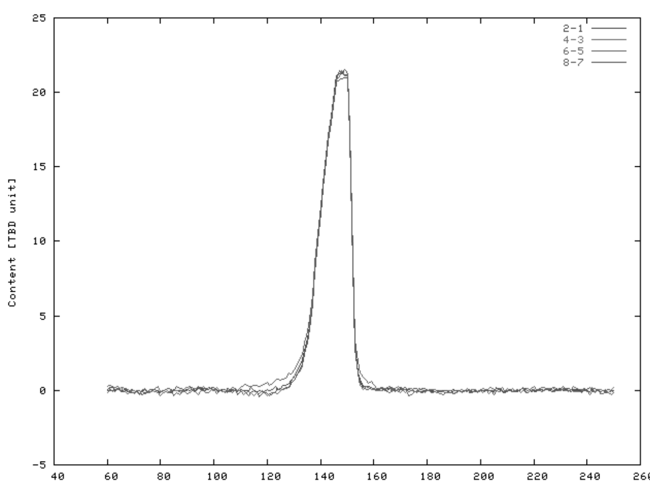

Figure 3.4-5: intensity variations after background subtraction and curve fitting

Unless the signal drifts during the time the measurements are taken, the behaviour cannot really be explained since one would expect the background subtraction to remove any slope. As this behaviour is still under investigation, no definite answer can be given yet, but it is expected that the signal is due to drifts in the sensor and sensor electronics. In depth knowledge of the exact camera build will therefore be necessary to determine the exact cause of this behaviour. For the moment however it is sufficient to conclude that it seems reasonable to remove the trend through curve fitting as this does not affect the actual signal.

3 NETD MEASUREMENTS

The NETD values measured have been measured on a single pixel without further averaging. If we calculate the expected NETD for a single pixel as derived for the MSI instrument we end up with the following calculation:

Required NETD	0.25 K
Signal gain through averaging of 7 samples (SQRT7)	2.65
Signal gain through averaging of 2 spectral bins (SQRT2)	1.41
Expected NETD	0.93 K

NOTE: this performance is predicted for a 40 mK NETD camera and an optical bench temperature of 230 K.

When compensating for a camera with 150 mK specified, the MIBS breadboard is **predicted** to have an NETD of **3.5 K** Preliminary **measurements** have shown a value of **3.7 K** so within the value predicted. Given the fact that there are still a number of issues unsolved like the lower then expected reflection of the mirrors used and the reported EMC problems [Ref1] as well as the fact that the breadboard has been operated significantly above 20 degrees and this is seen to have quite a large influence. We are confident that MIBS will meet the specifications as predicted in case the detector noise is improved and the bench is cooled down as originally anticipated.

4 CONCLUSIONS

At the moment the MIBS breadboard is under intensive evaluation, but for the moment a number of conclusions can be drawn.

- The breadboard is clearly capable of determining the 40 nm wavelength shift caused by the mode hopping of the used CO2 laser.
- Having large area's on the detector that are not influenced by signal properties helps to reduce bias and image fluctuation effects.
- The predicted sensitivity for the slit temperature has been clearly demonstrated
- The measured sensitivity to the camera temperature is more then expected, but this only helps for the actual instrument to meet the NETD specifications.
- For as far as can be concluded at this moment in time the MIBS breadboard meets the specifications and an Earthcare MSI instrument build in a similar way would meet the NETD specifications also.

As for the past, MIBS used to be part of the baseline for the Earthcare MSI instrument.
As for the present MIBS is under evaluation and until now performing as predicted.
As for the future we will stay in search for a flight opportunity that will allow us to prove the value of MIBS as a flight instrument.

Reference documents

[Ref1] Small Satellites for Earth Observation Berlin april 2007,IAA-B6-0304, Serious Microsats need serious instruments, MIBS and the first results. J.Leijtens et all.